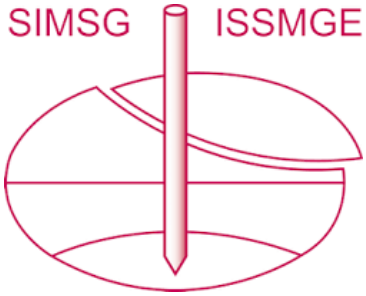
INTERNATIONAL SOCIETY FOR
SOIL MECHANICS AND
GEOTECHNICAL ENGINEERING



This paper was downloaded from the Online Library of the International Society for Soil Mechanics and Geotechnical Engineering (ISSMGE). The library is available here:

https://www.issmge.org/publications/online-library

This is an open-access database that archives thousands of papers published under the Auspices of the ISSMGE and maintained by the Innovation and Development Committee of ISSMGE.

The paper was published in the proceedings of the 6th International Conference on Geotechnical and Geophysical Site Characterization and was edited by Tamás Huszák, András Mahler and Edina Koch. The conference was originally scheduled to be held in Budapest, Hungary in 2020, but due to the COVID-19 pandemic, it was held online from September 26th to September 29th 2021.

Verification and modelling of seepage control walls

Zsombor Illés[1], Gábor Nagy[2]
Budapest University of Technology and Economics, Budapest, Hungary, zsombor.illes@epito.bme.hu[1], nagy.gabor@mail.bme.hu[2]

ABSTRACT: The main purpose of embankments is to protect the land which lies behind them from the effects acting on the waterside of the structure. To function as a safeguard, levees have to have two main features; (i) structural resistance and integrity, (ii) the retaining embankments have to have a certain level of water tightness. On the Great Hungarian plain dykes are usually constructed from local materials, which in many cases were not suitable for the purpose, furthermore they were insufficiently compacted. To increase the resistance of the ramparts, fly-ash based seepage control walls were constructed in thoroughly selected sections. In this paper, the properties of seepage control walls were examined, putting a great emphasis on the strength and permeability qualities of the structure. To construct a seepage control wall the soil of the embankments was stabilised with fly-ash based solder. Extensive experiments were carried out on the samples, which were from the southern part of the Great Hungarian plan. This paper deals with the samples from full scale mixed and stabilized seepage control walls and evaluates the results of the experiments. Moreover, cross sections were analysed with Plaxis 2D finite element software to evaluate the effect of seepage control wall in case of a flood and its significance on slope stability.

Keywords: soil stabilisation, fly ash, water retaining embankments, seepage control wall, finite element modelling

1. Introduction

The article is dealing with the strength and seepage properties of water retaining embankments. The core of these dykes were stabilised with a slag fly-ash based solder. The main function of dykes is to defend the land that lies behind them, from the floods coming from the waterside [1]. Against the water retaining embankments we set two main requirements, strength and water retaining properties [2]. The dyke system of Hungary bears the construction mistakes on itself from the XIX. century: (i) usage of unsuitable earthwork materials, (ii) inadequate compaction, (iii) built in cohesive soils with high water content, (iv) unfavourable subsoil conditions. The mentioned mistakes can appear alone and together at certain sections of the levees [3]. There are cases when the water permeability properties of some layers are not suitable, such as: intersection of an old riverbed, high organic content layers, thin layer of sand penetrates under the dyke, or inadequately compacted layers. In these cases, constructing a seepage control wall from the top of the embankment without demolishing the whole earthwork can be a sensible cost-efficient solution to increase defence properties of the embankment. Prior to the research presented here, at the Department of Engineering Geology and Geotechnics in BME experiments were conducted to optimise the soil-water-solder ratio for the most common soils used for dyke construction in Hungary [4]. After evaluating the results conclusions have been drawn and recommendations were made for the design and construction of such seepage control walls. In case of the sections analysed in this article the trench mix method was used.

1.1. Applied materials and technologies

There is an extensive literature for the application of slay and fly ash-based solders. The source of the fly ash can be coal fired power stations or municipal solid waste incineration (MSWI) fly as from different type of plants will differ [5]. A number of researchers dealt with the use of fly ash from incineration plants. Just to illustrate the scope of the problem, in Shanghai 50 000 ton of fly ash has been formed annually, the placement of it should be solved [6].

Fly ash is considered as a hazardous waste, because it has a heavy metal content that exceeds regulatory limits [7-8-9]. It may pollute the groundwater due to long term leaching in the landfill site. From there heavy metals became admissible and can enter the food chain. The pozzolanic material-based stabilisation of heavy metals in fly ash is a promising alternative, in this case the heavy metals are immobilised. In case of cement fly ash mixtures, the purpose of the second aggregate is to disperse, by this increasing the degree of hydration [10]. The aim of the researchers is to reduce the costly Portland cement used for soil stabilisation, because of that they experiment with the use of industrial by-products as a hydraulic binder. Calcium carbide residue (CCR) has a similar composition as hydrate lime, the stabilisation effect of the residue and fly ash was analysed on silty clay soils [11]. Similar to the authors of this article Sharma and Sivapullaiah [12] investigated the properties of slag-fly ash mixtures, they found out that if they added 2% lime to the 40% furnace slag, the binding process quickened and the samples had a denser structure.

1.1.1. Trench Mix Method

The Trench cutting and Remixing wall method is a relatively quick, clean and compact technique developed for constructing an engineered continuous in situ soil mix wall. The full-depth vertical cutter post resembles a giant chain saw; which vertically blends the entire soil profile with cement-based binder slurry added on site. Eliminating stratification and creating a near homogenous soil mix wall with low permeability, on the waterside the cut-off wall receives a HDPE foil. One of the big advantages of the process is that the soil is not removed from the

trench, just mixed with the binder reducing transportation and equipment costs, making in a clean and compact technique.

1.2. Overview of the treated earthworks

Close to 2000 meters of seepage control wall was constructed (Table 1.), from these walls approximately 30 m of undisturbed sample have been taken. Baks (1-3) explorations are at the embankments of the same stream but on different side. Baks 1-2 are at the right bank while Baks 3 is on the other side, at the left bank. Location of the settlement Baks is presented in **Error! Reference source not found.**., while the locations of the analysed cross sections are marked in Figure 1.

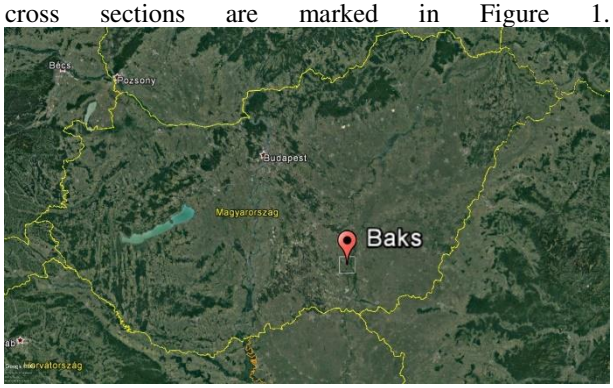


Figure 1. Location of Baks

Table 1. List of the sections analysed

Settlement near the site	Name of the location	Length of the cotoff wall [m]	Number of samples	Thickness of the cutoff wall in [cm]	Depth of the cutoff wall in [m]	Depth of the sample [m]
Baks	Baks1	956	1	40	8.00	8.00
	Baks2		1	40	8.00	8.00
Baks	Baks3	1000	1	40	9.00	9.00
Total length of the walls:		1956	3	Total length of borings:		25.00

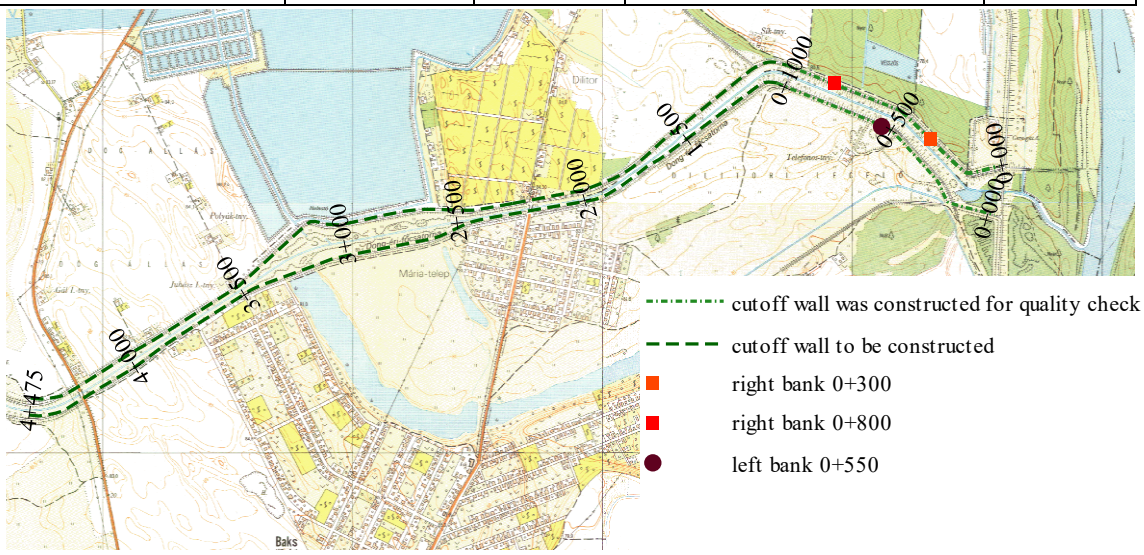


Figure 1. Location of the dykes and the analysed sections

1.2.1. Preliminary requirements for the seepage control walls

The strength properties of the samples were evaluated with uniaxial compression test according to the standard: MSZE CEN ISO/TS 17892-7:2010 [13]. Because the seepage control cut-off walls were mainly constructed in soft clays the confining pressure acting on them was neglacted. In case of the uniaxial compression strength tests, our expectation was that after homogenisation all the samples should have a higher compression strength than 300 kPa.

During the design phase of the full-scale soil stabilisation, cut-off wall construction, the permeability coefficient's maximum value was defined as $5 \cdot 10^{-7}$ m/s, according to the hungarian standard MSZ 15221 [14].

2. Strength parameters of the samples

First the seepage control walls' strength properties will be evaluated. The unconfined strength was determined by uniaxial compression test.

2.1. Stress-strain diagrams

Two figures containing stress-strain diagrams of the Baks 0+550 section are presented in Figure 2 and Figure 3.

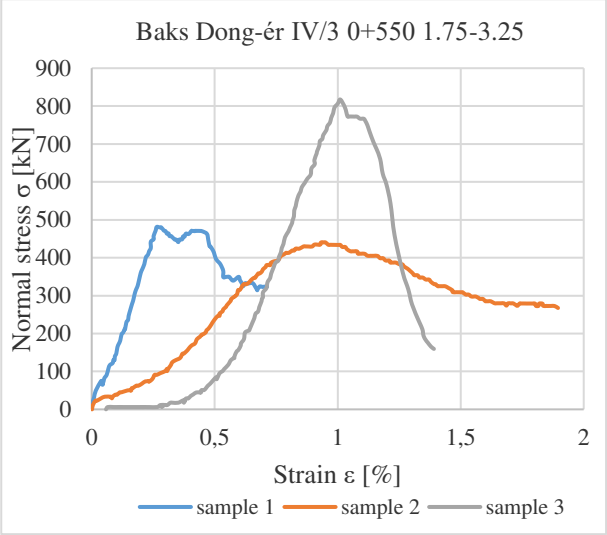


Figure 2. Stress-strain diagrams of Baks Dong-ér, section 0+550 depth 1.75-3.25m

In case of the upper part (1.75-3.25 m) of the cut-off wall, the samples behave more rigidly (Figure 2.), while in the lower parts (3.25-4.75) of the seepage control wall the samples have more residual strength. If the stress degradation is not so quick the failure mechanism is considered as plastic. In an event of failure there is time for the authorities to take action and ensure the section of the dyke which is about to burst.

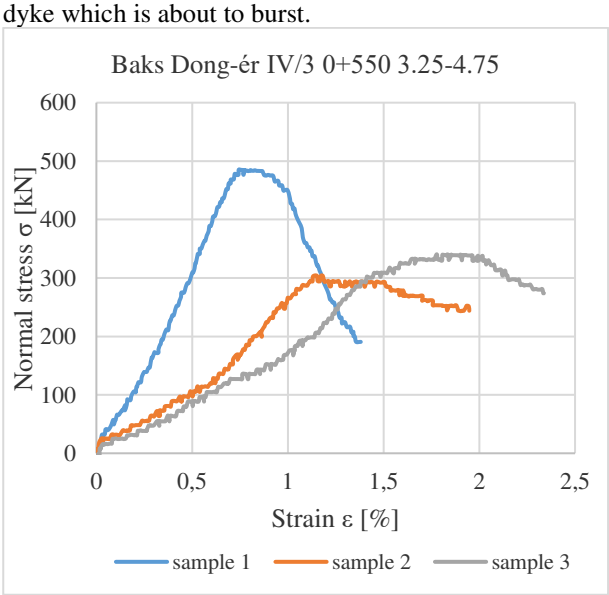


Figure 3. Stress-strain diagrams of Baks Dong-ér, section 0+550 depth 3.25-4.75m

2.2. Connection between the samples' void ratios and uniaxial strength

The three sections (Baks 1-3) void ratios in relation with the depth are presented in Figure 4.

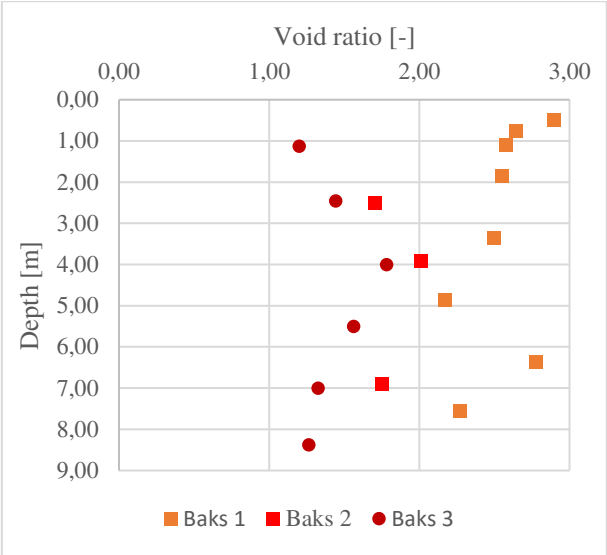


Figure 4. Void ratios of Baks sections 1 to 3

Error! Reference source not found.. summarises the mean values of void ratios (e) and normal stresses (σ), also provides statistical indicators such as standard deviation (Std.) and coefficient of variation (CV), which is also known as relative standard deviation. It is defined as the ratio of the standard deviation to the mean, expressed as a percentage.

	Baks 1		**Baks 2**		**Baks 3**	
	e [-]	**σ** [kPa]	**e** [-]	**σ** [kPa]	**e** [-]	**σ** [kPa]
Av.	2,50	**516,85**	1,82	302,85	1,43	297,37
Std.	0,240	158,26	0,165	124,47	0,216	164,69
CV %	9,60	**30,62**	**9,02**	41,10	15,11	55,38

All of the group of samples (Baks 1-3) have a low relative standard deviation for void ratio (e), which indicates that a fairly homogeneous seepage control wall was constructed. The average strength of the group of samples from Baks 2 is slightly above the appointed value (302.85>300.00) while in case of the Baks 3 group of samples it is just below (297.37<300.00). Furthermore, these samples strength properties have a high relative standard deviation (CV). The reason for it could be the high strength of the wall, which made hard the preparation of the samples, it also happened that inside the sample the HDPE foil appeared.

3. Evaluation of the seepage coefficient

Mentioned already in this article the maximum value for the seepage coefficient was defined as $5 \cdot 10^{-7}$ m/s. It was an important question whether the full scale samples have similar permeability properties as the small scale samples. The approximate characterisation of water movement in soil is based almost exclusively on Darcy's law [15] according to which the flow rate of water in soil can be discribed by the following relationship:

$$V = k \cdot i = k \cdot \frac{h}{l} \quad (1)$$

In Eq. (1), h is the hydraulic head between two points of a given flow line, l is the length of the flow line, i is the hydraulic gradient and k is the permeability coefficient of the soil.

The permeability coefficient of the soil was determined according to the following standard: ISO/TS 17892-11:2004 [16]. It is the only geotechnical parameter that varies within the widest range. Its value spans more than ten orders of magnitude. To define it is extremely important, but due to the fact that it stretches over more than ten orders of magnitude, only an order of magnitude estimation is possible. The permeability coefficient's order and the corresponding soil types are summarised in Table 2. Values of the permeability coefficient after Nagy [17]

Table 2. Values of the permeability coefficient after Nagy [17]

k (m/s)	10^{0}	10^{-1}	10^{-2}	10^{-3}	10^{-4}	10^{-5}	10^{-6}	10^{-7}	10^{-8}	10^{-9}	10^{-10}	10^{-11}	10^{-12}
Water conductivity	Very good			Good					Bad			Water tight	
Discription of the soil	Pebble stone	Gravel	Sandy gravel	Gravelly sands	Sand	Silty sand	Fine sand		Silt	Clay			

In Figure 5. each mark represents approximately a 1.5 m depth (0.75-2.25) of the seepage control wall. From each specimen 2-3 samples were spotted for the measurement of permeability coefficient. A total of 39 measurement was executed for 18 specimens.

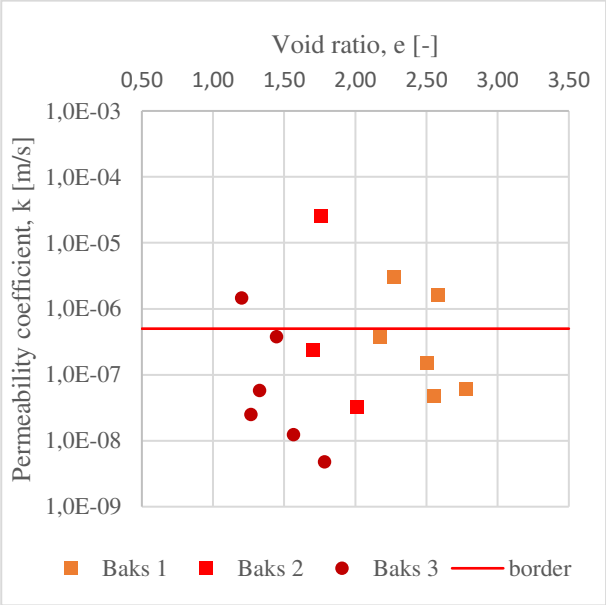


Figure 5. Permeability coefficients (k) of the Baks (1-3) sections

One or two specimens from every section have a higher permeability coefficient than the originally designed. In Figure 6. the permeability coefficients of Baks (1-3) sections are presented in a semi-logarithmic scale, in function of the depth. The contour of the seepage control wall (brown) and the contour of the embankment (green) also introduced. In two cases the permeability of the top 1.0 m was not adequate (Baks 1 and 3). Generally, the specimens from the top 2.0 m were very stiff, due to the likely accumulation of binder. It was very difficult to prepare proper samples with the methods used in soil mechanics for water permeability tests. For the lower permeability results at the base of the seepage control wall a likely reason is that the sampling boring was not exactly vertical, and it left the cut-off wall. At this level the seepage control wall was constructed in a silty sand layer which has a permeability around $2 \cdot 10^{-5}$ m/s.

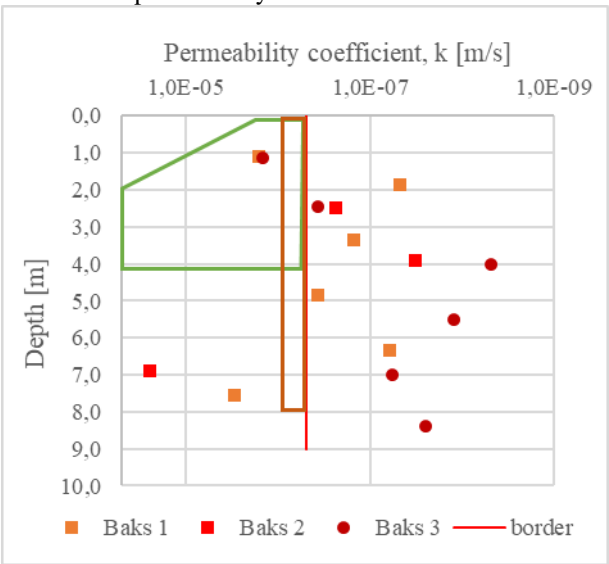


Figure 6. Permeability coefficients (k) of the Baks (1-3) sections relation to the depth

3.1. Some examples of the sampling

The permeability coefficient is very sensitive for the way the samples are prepared. The undisturbed samples arrived in 130 mm diameter PVC tubes, from these smaller 38 mm diameter and 75 mm height samples were spotted. If the specimens arriving to the laboratory were already fractured, it greatly increased the chances that the samples had also inherited these properties as well.

A sample in a good state is visible in Figure 7., while fissured and crumb state samples are visible in Figure 8. and Figure 9.



Figure 7. Proper undisturbed samples from Baks 2, Dong stream 0+550



Figure 8. HDPE foil in the undisturbed sample



Figure 9. Crumby sample

It should be emphasised that most of the samples arrived in a very good state, only a few were fractured, from these sections only one or two samples could be prepared for permeability test, which results should be treated with caution.

4. Finite element modelling of seepage through the cross section of Baks 0+550

The seepage calculation was done with Plaxis 2D finite element software. The following statements apply to the finite element model:

- horizontal layers were assumed based on the borehole made near the section;
- the dimensions of the constructed seepage control walls were taken from the drawings received from the designers;
- the waterway does not appear in the model, the seepage conditions are ensured by properly set boundary conditions.

In addition to the seepage modelling, the stability of the slope was also analysed. The calculations were carried out according to the basic principles of the Eurocode series of standards. According to Eurocode 7-1(MSZ EN 1997-1:2006) [18] design method 3 (DA-3), a combination of partial factor groups A2 "+" M2 "+" R3, shall be used to assess the overall stability of slopes and any geotechnical structure. In this case, the tests were carried out using the characteristic values of the soil parameters, and the final value of the "φ-c-reduction" method used for the stability tests of finite element programs gives the safety factor, which $\gamma\varphi' = \gamma c' = 1.35$, where $\gamma\varphi'$ refers to $\mathrm{tg}\varphi'$.

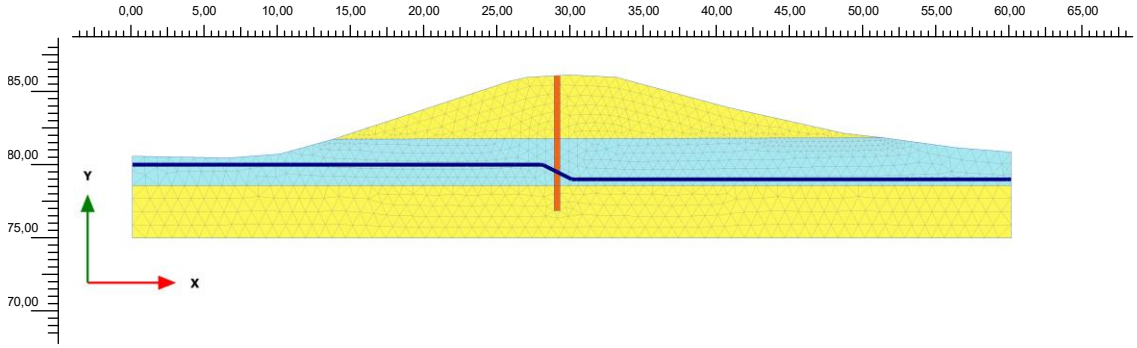


Figure 10. Connectivity plot (finit element mesh), of Baks 2 Dong stream, left bank, section 0+550

Table 3. Geotechnical properties of the materials

Baks 2, Dong stream, left bank, section 0+550				
Geotechnical parameter	Symbol	Soil type		
		Silty sand	Clay	Seepage control wall
Friction angle	ϕ (°)	18	3	5
Cohesion	c (kPa)	3	10	100
Oedometric Modulus	E_{oed} (kN/m^2)	8000	6000	16210
Wet unit weight	γ_w (kN/m^2)	18.50	19.00	21.00
Saturated unit weight	γ_s (kN/m^2)	19.50	20.00	23.00
Water permeability	k (m/sec)	1,89E-05	5,67E-07	3,23E-07
	k (m/day)	1,63E+00	4,90E-02	2,79E-02

The problem was solved as a 2D Plain Strain model using 15-node triangles [19]. The finite element mesh generated by the software is shown in Figure 10. The yellow layer is silty sand, while the turquoise blue is the clay. The activated seepage control wall is coloured orange on the plot. The dark blue line represents the initial phreatic level. The soil properties are summarised in Table 3.

During the calculation the following phases were defined in the model:

1. Initial phase (Gravity loading),
2. Initial phase (Plastic calculation)
3. Seepage calculation without cut-off wall (Fully coupled flow-deformation),
4. Stability analysis without cut-off wall (Safety calculation),
5. Seepage calculation after the construction of cut-off wall (Fully coupled flow-deformation),
6. Stability analysis after the construction of cut-off wall (Safety calculation).

4.1. Seepage analysis, with and without cut-off wall

The pore water pressure at the peak of the flood wave is shown in Figure 11. without the seepage control wall. As the wall is not yet installed, the flow of water is free. The effect of the construction of the cut-off wall is shown in Figure 12., which inhibits the increase in pore water inside and behind the wall.

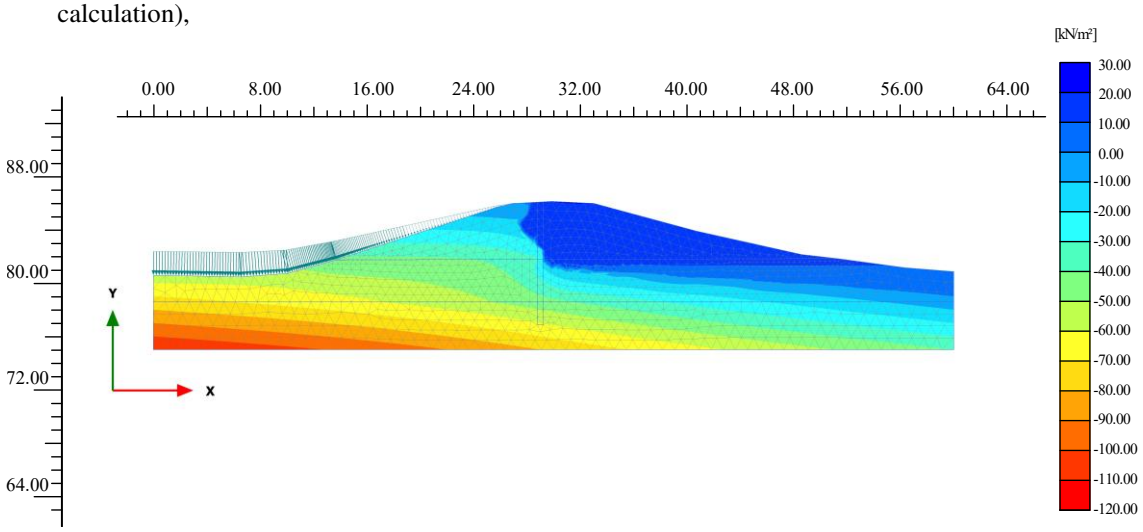


Figure 11. Pore water pressure distribution without the seepage control wall, Baks 2, Dong stream left bank 0+550

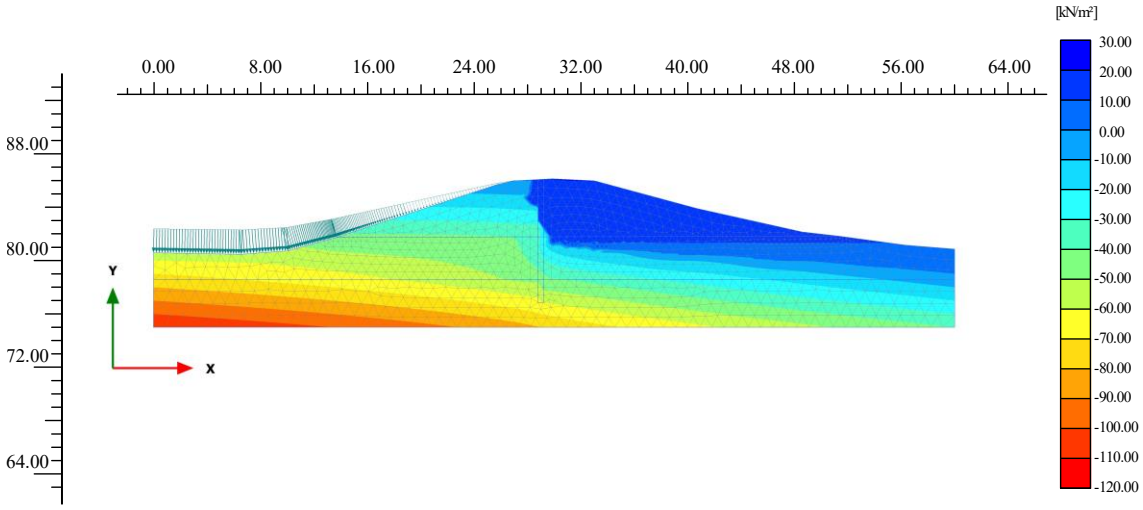


Figure 12. Pore water pressure distribution after the construction of the seepage control wall, Baks 2, Dong stream left bank 0+550

4.2. Stability analysis, with and without cut-off wall

The critical slip surface develops on the land side of flood protection embankment. Figure 13. shows a critical slip surface without the cut-off wall from and Figure 14. shows a critical slip surface after the seepage control wall has been installed. The cut-off wall prevents the critical slip surface from being cut out on the waterside.

The safety factor of the land side slope (ΣM_{sf}) increased from the original 1.893 to 1.940.

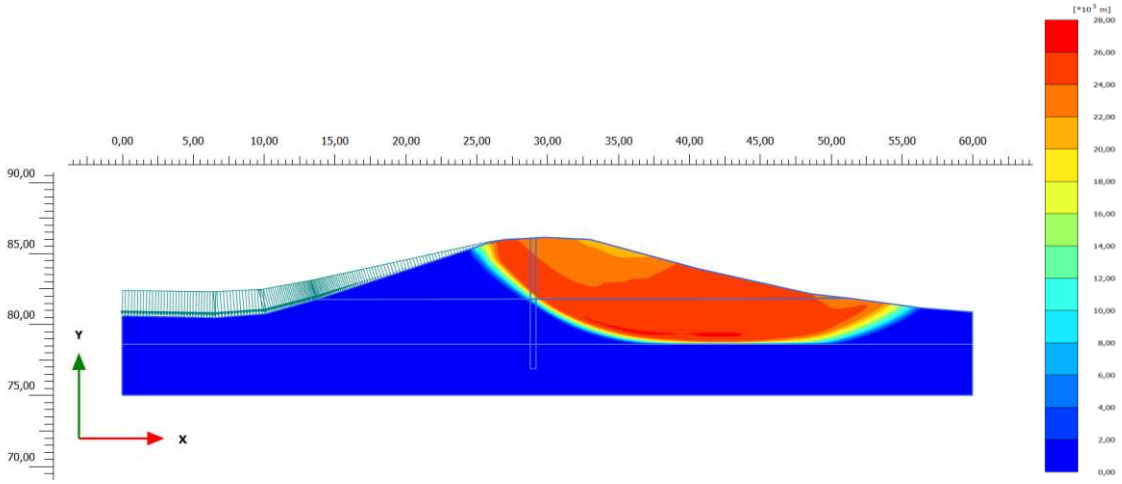


Figure 13. Critical slip surface without the cut-off wall

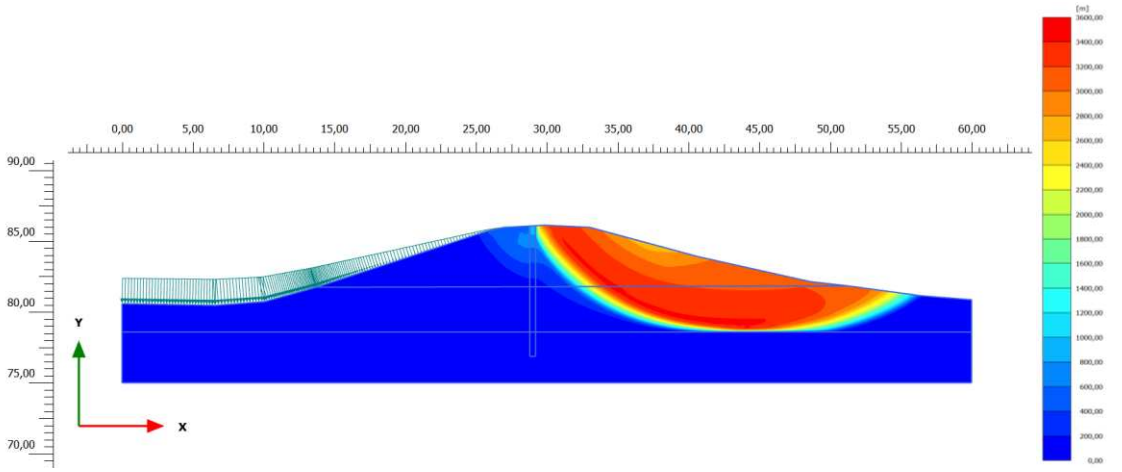


Figure 14. Critical slip surface after the seepage control wall has been installed

5. Conclusions

Most of the flood protection embankments in the Great Plain are made of local materials. A lot of mistakes were made during the construction, such as: poor soil quality, lack of compaction, high water content of cohesive soils, neglection of subsoil condition during design phase of the embankments. When the embankments were strengthened proper adhesion had not been provided between the layers. To correct many of these mistakes the construction of seepage control wall can be a proper solution, which increases the length of the seepage path and strengthen the slopes. The degree of improvement depends on the structure and stratification of the embankment, furthermore on the depth of the cut-off wall.

The key findings about the seepage control walls can be summarised as follows:

- Homogeneous structures can be formed during the construction of seepage control walls, the strength and permeability characteristics do not change significantly with depth.
- In case of the strength properties the appointed aim was achieved. The unconfiend strength of the soil reached 300 kPa and exceeded it in most of the cases.
- The value of the permeability coefficient in the cut-off wall is independent of the depth since homogeneous design was sought and achieved when the walls were created by mixing the soil of the embankment with solder. The seepage coefficient of $5 \cdot 10^{-7}$ m/s determined based on MSZ 15221 and was fulfilled by the examined levee sections.

Acknowledgement

The authors would like to express their gratitude for Professor László Nagy, who followed the research from the initial stage and supported the authors with his endless ideas and advices.

References

[1] L. Nagy, 'Dike breaches in the Carpathian basin', *Periodica Polytechnica Civil Engineering*, vol. 50, no. 2, pp. 115–124, 2006.

[2] L. Nagy, 'Estimating Dike Breach Length from Historical Data', *Periodica Polytechnica Civil Engineering*, vol. 50, no. 2, pp. 125–139, 2006.

[3] L. Nagy, ‘Az árvízvédelmi gátak geotechnikai problémái’, *Vízügyi Közlemények*, vol. 82, no. 1, pp. 121–146, 2000.
[4] R. Nagy and G. Nagy, ‘Agyagtalaj stabilizációja pernyével’, in *Török, Ákos; Görög, Péter; Vásárhelyi, Balázs (szerk.) Mérnökgeológia -Kőzetmechanika 2015*, Budapest, Hungary, 2015, pp. 347–354.
[5] X. Wang, A. Li, and Z. Zhang, ‘The Effects of Water Washing on Cement-based Stabilization of MWSI Fly Ash’, *Procedia Environmental Sciences*, vol. 31, pp. 440–446, 2016, doi: 10.1016/j.proenv.2016.02.095.
[6] L. Xinying, C. Quanyuan, and Z. Yasu, ‘Stabilization of heavy metals in MSWI fly ash using silica fume’, *Journal of Waste Management*, vol. 34, pp. 2494–2504, 2014.
[7] J. Yvon *et al.*, ‘Long-term stability in landfills of Municipal Solid Waste Incineration fly ashes solidified/stabilized by hydraulic binders’, *Journal of Geochemical Exploration*, vol. 90, no. 1–2, pp. 143–155, Jul. 2006, doi: 10.1016/j.gexplo.2005.09.008.
[8] H. Shi and L. Kan, ‘Characteristics of municipal solid wastes incineration (MSWI) fly ash–cement matrices and effect of mineral admixtures on composite system’, *Construction and Building Materials*, vol. 23, no. 6, pp. 2160–2166, Jun. 2009, doi: 10.1016/j.conbuildmat.2008.12.016.
[9] R. Yang, W.-P. Liao, and P.-H. Wu, ‘Basic characteristics of leachate produced by various washing processes for MSWI ashes in Taiwan’, *Journal of Environmental Management*, vol. 104, pp. 67–76, Aug. 2012, doi: 10.1016/j.jenvman.2012.03.008.
[10] S. Horpibulsuk, R. Rachan, and Y. Rakschon, ‘Role of fly ash on strength and microstructure development in blended cement stabilized silty clay’, *Soils and Foundations*, vol. 49, no. 1, pp. 85–98, 2009.
[11] S. Horpibulsuk, C. Phetchuay, A. Chinkulkijniwat, and A. Cholaphatsorn, ‘Strength development in silty clay stabilized with calcium carbide residue and fly ash’, *Soils and Foundations*, vol. 53, no. 4, pp. 477–486, Aug. 2013, doi: 10.1016/j.sandf.2013.06.001.
[12] A. K. Sharma and P. V. Sivapullaiah, ‘Strength development in fly ash and slag mixtures with lime’, *Proceedings of the Institution of Civil Engineers - Ground Improvement*, vol. 169, no. 3, pp. 194–205, Aug. 2016, doi: 10.1680/jgrim.14.00024.
[13] European committee for standardization, *Unconfined compression test on fine-grained soils (ISO/TS 17892-7:2004)*, vol. 7, 12 vols. Brussels, 2004.
[14] European committee for standardization, *Facility Management. Part 2: Guidance on how to prepare Facility Management agreements MSZ EN 15221-2:2007*, vol. 2, 2 vols. Brussels, 2007.
[15] H. Darcy, *Les Fontaines Pbliques de la Ville de Dijon*. Paris, France, 1856.
[16] European committee for standardization, *Determination of permeability by constant and falling head (ISO/TS 17892-11:2004)*, vol. 11, 12 vols. Brussels, 2004.
[17] L. Nagy, *Árvízvédekezés a településeken*. Budapest, Hungary, 2010.
[18] European committee for standardization, *Eurocode 7: Geotechnical design. Part 1: General rules*. Brussels, 2006.
[19] Bentley, *Plaxis 2D Reference Manual*. 2016.